A Spectrum Surveying Framework for Dynamic Spectrum Access Networks

Dinesh Datla, *Student Member, IEEE*, Alexander M. Wyglinski, *Member, IEEE*, and Gary J. Minden, *Senior Member, IEEE*

***Abstract*—Dynamic spectrum access networks and wireless spectrum policy reforms heavily rely on accurate spectrum utilization statistics, which are obtained via spectrum surveys. In this paper, we propose a generic spectrum-surveying framework that introduces both standardization and automation to this process, as well as enables a distributed approach to spectrum surveying. The proposed framework outlines procedures for the collection, analysis, and modeling of spectrum measurements. Furthermore, we propose two techniques for processing spectrum data without the need for *a priori* knowledge. In addition, these techniques overcome the challenges associated with spectrum data processing, such as a large dynamic range of signals and the variation of the signal-to-noise ratio across the spectrum. Finally, we present mathematical tools for the analysis and extraction of important spectrum occupancy parameters. The proposed processing techniques have been validated using empirical spectrum measurements collected from the FM, television (TV), cellular, and paging bands. Results show that the primary signals in the FM band can be classified with a miss-detection rate of about 2% at the cost of 50% false-alarm rate, while nearly 100% reliability in classification can be achieved with the other bands. However, the classification accuracy depends on the duration and the range of frequencies over which data are collected, as well as the RF characteristics of the spectrum measurement receiver.**

***Index Terms*—Characterization of spectrum, dynamic spectrum access (DSA) networks, measurement data classification, spectrum measurements, spectrum sensing.**

I. Introduction

THE DYNAMIC nature of spectrum behavior poses a challenge to the implementation of *dynamic spectrum access* (DSA) networks. This is due to the fact that the spectrum behavior can vary as a function of frequency, time of radio operation, geographical location, and other features [1]. Furthermore, the unlicensed (i.e., secondary) user spectrum access may encounter incumbent licensed (i.e., primary) users that possess different transmission characteristics [2]. To counter these challenges and operate in a manner that is transparent to the incumbent primary users, the radio must adapt to the varying spectrum operating conditions. Hence, a thorough understanding of the spectrum can aid in the effective design and execution of interference-free DSA technologies. To obtain this knowledge, surveying of the spectrum activity can be conducted, which mainly involves the processing and analysis of spectrum measurements.

Although several spectrum surveys have been presented in the literature [3]–[7], a formalized mathematical framework for spectrum surveying is currently unavailable. A mathematical framework would provide in-depth understanding of the spectrum surveying process, enabling the optimization of the spectrum surveying process. Such a framework can also be incorporated into real-time mechanisms, thus enabling DSA networks to identify potential opportunities for secondary access [8].

Spectrum measurements are processed to remove defects introduced by noise and intermodulation [5], as well as for measurement data processing. The processed data can then be analyzed to characterize the spectrum occupancy, which is useful for applications such as interference analysis [9]. In addition, the unused spectrum can be quantified to assess the feasibility of DSA operation [6]. The data analysis can also be performed to build spectrum models that facilitate long-term and short-term forecasting of spectrum occupancy [10]–[12], as well as form the basis for adaptive DSA protocols [8].

Among the various signal detection techniques presented in the literature [13], *energy detection* is the optimal method when only power measurements are available [14]. In energy detection, the measurements that occur above a decision threshold are identified as signal power samples. This threshold can empirically be determined via visual inspection of the spectrum data [2], [7] or be computed as a function of several receiver properties such as the noise floor [2], [6]. This threshold can also be estimated based on the analysis of a noise histogram [5], [15] or a spectrum data histogram [1]. However, these methods possess some drawbacks. For instance, threshold estimation by empirical analysis cannot be implemented in an automated manner. Moreover, the estimated threshold is receiver specific, while some of the methods require *a priori* knowledge of the noise statistics for the threshold estimation. Finally, these

Manuscript received July 24, 2008; revised January 13, 2009 and March 22, 2009. First published April 24, 2009; current version published October 2, 2009. This work was supported by the National Science Foundation under Grant ANI-0230786 and Grant ANI-0335272. This paper was presented in part at the IEEE International Symposium on New Frontiers in Dynamic Spectrum Access Networks, Baltimore, MD, November 2005. The review of this paper was coordinated by Dr. H. Jiang.

D. Datla was with the Information and Telecommunication Technology Center, University of Kansas, Lawrence, KS 66045-7612 USA. He is now with the Department of Electrical and Computer Engineering, Virginia Polytechnic Institute and State University, Blacksburg, VA 24061 USA (e-mail: ddatla@vt.edu).

A. M. Wyglinski was with the Information and Telecommunication Technology Center, University of Kansas, Lawrence, KS 66045-7612 USA. He is now with the Department of Electrical and Computer Engineering, Worcester Polytechnic Institute, Worcester, MA 01609-2280 USA (e-mail: alexw@wpi.edu).

G. J. Minden is with the Information and Telecommunication Technology Center at the University of Kansas, Lawrence, KS 66045-7612 USA (e-mail: gminden@ittc.ku.edu).

Color versions of one or more of the figures in this paper are available online at http://ieeexplore.ieee.org.

Digital Object Identifier 10.1109/TVT.2009.2021601

methods do not perform well when the noise power varies across the spectrum.

In addition to these drawbacks, there exist several challenges to performing measurement data classification: First, there can be some overlap between the histograms of the signal[1] and noise samples in the spectrum data. Across the range of measurement values over which the histograms overlap, there can be ambiguity in the measurement data classification. Consequently, this overlap results in a tradeoff between the miss-detection rate and the false-alarm rate when setting the threshold. Second, variations in the noise power levels and the SNRs across the spectrum may occur. Third, signals may be received from both distant and nearby transmitters. Due to the high dynamic range of the signals, the stronger signals may bias the threshold estimation process, and this phenomenon can be termed as the *biasing effect*. Due to the biasing effect, the resulting threshold may be so high that weak signals may not be detected.

In this paper, we propose the *spectrum survey framework* (SSF), which standardizes the spectrum surveying process by providing a layout for the different stages of the survey, as well as defining the procedures involved at each stage in a convenient mathematical form. Standardization of the spectrum surveying process can provide a uniform basis for the collaborative study of spectrum utilization. Collaborations on collecting and analyzing spectrum measurements overcome the limitations of localized spectrum utilization studies. We also propose two measurement classification methods to counter the challenges to measurement classification, such as the biasing effect and nonuniform noise power levels. The proposed methods can estimate the decision threshold based on the statistical properties of the spectrum data, without requiring any *a priori* knowledge. In addition, mathematical procedures for analyzing the data to gain useful information on spectrum utilization are presented. Finally, a model for spectrum measurements is proposed.

The rest of this paper is organized as follows. In Section II, the proposed SSF is presented along with its implementation. The proposed spectrum data processing methods are presented in Sections III. Section IV provides details on spectrum data analysis and modeling. The results of applying the proposed processing methods on spectrum data are displayed in Section V. Section VI presents several concluding remarks.

II. Spectrum Survey Framework

A spectrum survey generally consists of three stages: 1) The occupancy in the target spectrum is captured by collecting spectrum measurements, with the measurement data archived in a suitable format; 2) the spectrum data are processed to distinguish the signal and noise measurements; the processed data are then analyzed to extract the characteristics of the spectrum utilization from the measurements; and 3) the occupancy in the target spectrum is modeled for further analysis. The proposed SSF provides a layout that maintains the sequential order

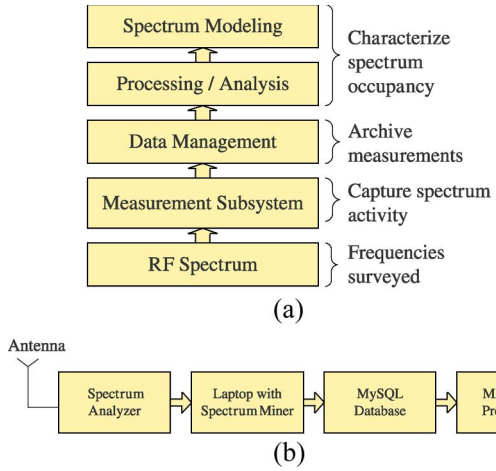

Fig. 1. Block diagrams of the proposed SSF. (a) High-level structure of SSF. (b) Implementation of SSF.

of occurrence of the different stages of spectrum surveying, as shown in Fig. 1(a). It also provides standardized procedures for recording, storing, and sharing the measurements with the research community. Finally, it enables an automated and efficient approach for spectrum surveying.

In the framework, the *measurement subsystem* is responsible for collecting the spectrum measurements. The *data management* block formats the measurement data and transfers it to a storage device or to a centralized database where it can be archived for future processing. This block facilitates distributed spectrum surveying and enables collaborations on the study of the spectrum by supporting distributed and simultaneous data collection as well as providing a mechanism to easily share data among researchers. For instance, the archived data can be published to the research community via the World Wide Web. In the *processing and analysis* block, statistical methods are used to process the data. The information about the spectrum utilization, which is retrieved by performing analysis on the processed data, is used to model the spectrum behavior in the *modeling* block. Together, the processing and analysis block and the modeling block perform the characterization of the spectrum behavior.

Our prototype of the proposed SSF is shown in Fig. 1(b). In our measurement campaign, an HP 8594E spectrum analyzer was employed as the measurement subsystem, while the *Spectrum Miner*[2] software was used to automate the collection and storage of spectrum measurements. It includes a graphical user interface that allows for the various parameters of the measurement subsystem to be set and a software module that controls the measurement subsystem based on the set parameters. The software is also responsible for formatting the spectrum data and storing them in a database. The measurements can be exported from the database into an analysis tool such as Matlab or Mathematica, as well as archived in a web-based spectrum data repository.

Each of the blocks in SSF, with the exception of the data management block, is described in detail in the following

[1]The signal being referred here is not a pure signal but contains noise added to it.

[2]The Spectrum Miner software has been developed in-house at the University of Kansas by T. Weidling and R. Petty.

sections. Reference [1] gives more details on the architecture of the Spectrum Miner software and the data-management block. In the measurement subsystem, there are several parameters of spectrum sensing that need to be considered for collecting the measurements, which are discussed next.

A. Measurement Subsystem and Parameters of Spectrum Sensing

The primary dimensions of the spectrum are frequency, time, spatial extent, and signal format [1]. The frequency and time attributes refer to the frequency of the RF energy and the time that it occurs. Spatial extent is the spatial volume that the receiver senses, which can be specified by the geographical location of the receiver (location type: urban, suburban, or rural), the angle of arrival (azimuth) of the signal, and the beam pattern of the antenna. Theoretically, if an isotropic antenna is used, the spatial extent is a sphere around the receive antenna. The signal format can be specified in terms of the type of polarization and modulation. It accounts for the use of orthogonal signal spaces, such as horizontal polarization, vertical polarization, and code space.[3]

In our spectrum survey, the measurements were taken with a single omnidirectional antenna; therefore, the spatial extent is not relevant since the angle of arrival cannot be resolved. The measurements only include the power of the received signal. As a result, the signal format is not relevant as well since the power measurements do not convey any information about the polarization of the signal, and we do not attempt to despread if the signal is based on spread spectrum. Thus, from our measurements, we can only resolve the spectrum occupancy along the frequency and time dimensions. Accordingly, a set of measurements that are collected along a frequency range and over a period of time can be represented by an $N_t \times N_f$ matrix $\mathbf{M}$ as

$$\mathbf{M} = [M(f_i, t_j)]$$

where

$$\begin{aligned} F_{\text{start}} \leq f_i < F_{\text{stop}} \\ T_{\text{start}} \leq t_j < T_{\text{stop}} \\ i = 1, \ldots, N_f; \quad j = 1, \ldots, N_t \end{aligned} \tag{1}$$

given that $M(f_i, t_j)$ is a sample of the RF power [expressed in decibels referenced to 1 mW (dBm)] residing in the frequency channel f_i at time instance t_j, F_{start} and F_{stop} specify the start and stop frequencies for the measurement sweep, T_{start} and T_{stop} specify the start and stop time instances for the sweep, and N_t and N_f are the number of time instances and frequency channels from which the measurements are collected. We can represent a submatrix of $\mathbf{M}$ by $\mathbf{M}_{F,T}$, which is defined over a range of frequencies and time instances specified by F and T, where F represents a subrange of $[F_{\text{start}}, \ldots, F_{\text{stop}})$, and T represents a subrange of $[T_{\text{start}}, \ldots, T_{\text{stop}})$.

During a measurement test, the spectrum measurement equipment scans across the *sweep bandwidth* B_s in steps of the bandwidth resolution B_r. Accordingly, the frequencies that are scanned in a single sweep can be represented as

$$f_i = F_{\text{start}} + ((i-1) \times B_r), \qquad i = 1, \ldots, N_f \tag{2}$$

where

$$N_f = \frac{B_s}{B_r} \tag{3}$$

$$B_s = F_{\text{stop}} - F_{\text{start}}. \tag{4}$$

Every time the sweep bandwidth B_s is scanned, we can imagine that a bandpass filter of bandwidth B_d is stepped in frequency increments of B_r, where B_d is referred to as the *binwidth*. At each frequency step, B_d is centered about frequency f_i, and the measurements are collected for a duration of T_d, which is the *dwell time* [10]. The average of the measurements collected across B_d over time T_d is stored as the power at that frequency channel, which is represented as

$$M(f_i, t_j) = \frac{1}{B_d T_d} \times \int_{t_j - \frac{T_d}{2}}^{t_j + \frac{T_d}{2}} \int_{f_i - \frac{B_d}{2}}^{f_i + \frac{B_d}{2}} P(f, t)\, df\, dt \tag{5}$$

where $P(f, t)$ represents the measured power spectral density, and f and t are continuous variables of frequency and time, respectively. For statistical independence of measurements collected from two adjacent channels, the condition that $B_d \leq B_r$ has to be satisfied.

The *sweep time* T_s, which is the total time taken to complete a single sweep across B_s, is expressed as

$$T_s = (N_f T_d) + T_a. \tag{6}$$

In (6), in addition to the scanning time, additional delay T_a is introduced by the software that controls the sweep parameters and the data management block that transfers the data through buffers to the database. The total time for which the measurement test is conducted is denoted by T. Since T_s is finite, the instantaneous power in a frequency channel is measured in steps of the *sweep time resolution* T_r as

$$t_j = T_{\text{start}} + ((j-1) \times T_r) \tag{7}$$

where

$$j = 1, \ldots, N_t \tag{8}$$

$$N_t = \frac{T}{T_r}, \qquad T = T_{\text{stop}} - T_{\text{start}} \tag{9}$$

$$T_r \propto T_s. \tag{10}$$

Intuitively, the inverse relationship between T_s and B_r results in a tradeoff between them.

A measurement sweep can be specified by T, B_s (F_{start}, F_{stop}), B_d, and B_r. After assigning suitable values to these parameters, a measurement test is set up and conducted to collect measurements. The collected measurements have to be processed prior to performing the analysis.

[3]This is achieved using spreading codes.

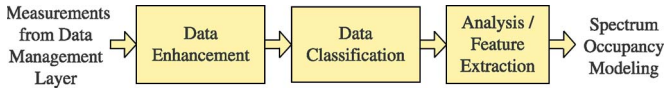

Fig. 2. Stages involved in the processing and analysis of spectrum measurements.

III. Spectrum Data Processing

Once the spectrum measurements have been obtained and stored in the database, the spectrum data can be retrieved at a later time for processing and analysis. Fig. 2 presents the block diagram of the different stages involved in the processing and analysis block of the SSF. Initially, preprocessing operations involving data enhancement are performed on the data, followed by spectrum classification of the data. Data enhancement is performed to refine the data and make them more suitable for the following classification process.

Let the preprocessed data be represented as $\mathbf{M}_{\mathrm{p}} = [M_p(f_i, t_j)]$. In the enhanced data matrix $\mathbf{M}_{\mathrm{p}}$, each element $M_p(f_i, t_j)$ is classified either as a signal (denoted by "1") or noise (represented as "0"), based on a decision threshold η

$$M_c(f_i, t_j) = \left\{ \begin{array}{ll} 1, & M_p(f_i, t_j) \geq \eta \\ 0, & M_p(f_i, t_j) < \eta \end{array} \right\} \tag{11}$$

where the *spectrum availability function* $\mathbf{M}_c = [M_c(f_i, t_j)]$ represents the matrix of classifications. The threshold can be an estimate of the average noise power where the spectrum measurements exceeding this threshold are classified as signals. The threshold needs to be optimum to perform classification with a minimum number of errors.

To counter the challenges involved in spectrum data processing, we use the following techniques for spectrum data processing: optimum thresholding using Otsu's algorithm [16], data enhancement and noise suppression [17], recursive thresholding [18], and adaptive thresholding [17]. Otsu's algorithm computes an optimum threshold that results in the maximum separation between the histograms of the signal and noise samples in the data [16]. Recursive thresholding and adaptive thresholding can be used to counter the challenges due to the high dynamic range of signals and the nonuniform power levels.

A. Spectrum Data Preprocessing

By suppressing the noise without affecting the signals, the histogram of noise samples is shifted to lower power levels such that the overlap in the histograms[4] of the signal and noise samples is reduced. This increased separation of the histograms can result in less-erroneous classification of the spectrum data. The measurement data can be refined by clipping, contrast manipulation, low-pass filtering, and time averaging. Whereas the latter two processing techniques can be performed on the data in their original form, the former two processing techniques are performed on their gray-scale values.

Clipping away the strong signals and the low noise powers can result in the reduction of the dynamic range of the measurements, while amplitude scaling can be performed to increase the contrast between the signals and noise. It is first assumed that the leftmost (i.e., the lower power levels) and the rightmost (i.e., higher power levels) portions of the spectrum data histogram contain only noise and signal power samples, respectively. With this assumption, the gray-scale values of the measurements that occur above and below the gray levels η_r and η_l are clipped at their respective thresholds, while the gray values that occur within the range of $(\eta_l, \ldots, \eta_r)$ are scaled to the range $[0.0, \ldots, 1.0]$, as shown in (12). Equation (13) represents the contrast manipulation process. In this manner, the clipping operation is combined with contrast manipulation as

$$I_p(f_i, t_j) = \left\{ \begin{array}{ll} \eta_r, & I(f_i, t_j) \geq \eta_r \\ p, & \eta_l < I(f_i, t_j) < \eta_r \\ \eta_l, & I(f_i, t_j) \leq \eta_l \end{array} \right\} \tag{12}$$

where

$$p = \frac{I(f_i, t_j) - \eta_l}{\eta_r - \eta_l} \tag{13}$$

$$I(f_i, t_j) = \frac{M(f_i, t_j) - \min\{\mathbf{M}\}}{\max\{\mathbf{M}\} - \min\{\mathbf{M}\}}, \qquad M(f_i, t_j) \in \mathbf{M} \tag{14}$$

$$0.0 < \eta_l, \eta_r < 1.0 \tag{15}$$

where $I(f_i, t_j)$ is the gray-scale equivalent of $M(f_i, t_j)$, which is computed using a linear transformation, as shown in (13), and $I_p(f_i, t_j)$ is the processed gray-scale measurement sample.

The noise that occurs as high-variance components in the spectrum data is suppressed by low-pass filtering the data in $\mathbf{I}$ using the averaging filter and the Gaussian low-pass filter [17].[5] Noise variance can also be reduced by averaging over several sweeps of data. In certain bands with fixed channelization, such as the FM and television (TV) broadcast bands, most active licensees continuously transmit for 24 h. In such cases, all the measurement sweeps of data collected across a band represent redundant data. By averaging over such redundant sweeps of data, which are affected by independent random noise, the noise variance is reduced. However, this method may not be effective when applied to bands occupied by bursty signals. The average power at frequency f_i can be computed from the measurements as

$$M_a(f_i) = \frac{1}{N_t} \sum_{j=1}^{N_t} M(f_i, t_j) \qquad \text{where} \quad F_{\mathrm{start}} \leq f_i < F_{\mathrm{stop}}. \tag{16}$$

Occasionally, some of the outputs of the classification process may contain signal samples that appear as isolated and scattered grains in the gray-scale intensity plot of the classified data. These signals could potentially be noise samples that have wrongly been classified as signals. As a result, median filtering [17] can be performed to remove these grains and reduce the false-alarm rate. The preprocessed data are provided as input to the classification algorithms that are presented next.

[4]We model the distributions of the signal and noise samples in the spectrum data with histograms, which overlap due to the presence of weak signals.

[5]The Matlab built-in functions for Otsu's algorithm, the Gaussian low-pass filter, and the median filter have been used for the processing.

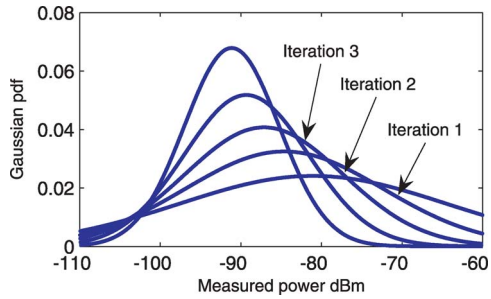

Fig. 3. Normal distribution of measurement samples to illustrate the first four iterations of the ROHT algorithm for a 99% confidence interval.

B. Proposed Classification of Spectrum Measurements

Recursive thresholding classification is suitable for detecting signals with a wide range of power levels. The adaptive thresholding algorithm presented in this paper is more generic than the algorithm presented in [2]. In Sections III-B1 and 2, the proposed algorithms for recursive thresholding and adaptive thresholding are described.

1) ROHT Algorithm: The proposed *recursive one-sided hypothesis testing* (ROHT) algorithm operates based on the concept of one-sided hypothesis testing [19]. This algorithm operates by making the assumption that the measurement data follow a Gaussian distribution and that there are a sufficient number of measurement samples such that the estimates of the mean and standard deviation obtained from the data are accurate.

At every iteration, a percentage of the measurements (specified by the z-value)[6] on the far right of the Gaussian distribution are identified as signals. The signal portion is discarded, and this process is iteratively repeated on the remaining unclassified measurements. As shown in Fig. 3,[7] after every iteration, the standard deviation is reduced. The algorithm stops iterating when the change in the standard deviation between two consecutive iterations becomes less than or equal to ϵ, where ϵ is an arbitrary positive value that is specified.

Let S be the set of signals within $\mathbf{M}$, S_k be a subset of S for the kth iteration of the algorithm, Q be the set of noise samples within $\mathbf{M}$, Q_k be a superset of Q for the kth iteration (Q_k may contain signals), μ_k and σ_k be the mean and standard deviation of the elements of Q_k, and θ_k be the decision threshold to identify the signal portion for the kth iteration. The algorithm is mathematically represented by the following pseudocode.

Initialize $S = \oslash$, $S_o = \oslash$, $Q_o = \mathbf{M}$, q
do
1) $\theta_{k+1} = z\text{-value} * \sigma_k + \mu_k$
2) $S_{k+1} = \{q_k \,|\, q_k \in Q_k, q_k \geq \theta_k\}$
3) $Q_{k+1} = Q_k - S_{k+1}$ (set subtraction)
4) $S = S \cup S_{k+1}$
5) $k = k + 1$
Until $(\sigma_{k-1} - \sigma_k) \leq \epsilon$

[6]The z-value is the number of standard deviations away from the mean in a distribution. It is related to the confidence level [20].

[7]The Gaussian curves have been generated from the statistics of the FM band (88–108-MHz) measurements after every iteration of the ROHT algorithm and not directly generated from the data. These curves illustrate the working of the ROHT algorithm.

By discarding the stronger signals at every iteration, their biasing effect on the weaker signals is greatly reduced. After each iteration, an improvement in the miss rate can be obtained but at the cost of an increase in the false-alarm rate.

One drawback with this algorithm is that not all distributions are Gaussian. Furthermore, the central limit theorem is applicable only when there are a large number of samples available such that the actual distribution converges to the Gaussian distribution.

2) Sliding-Window Adaptive Thresholding: A global threshold may not be optimum for the entire set of measurements, particularly when the noise and signal statistics vary across the spectrum. In this case, spectrum classification can be performed using local threshold values that vary over the measurement set as a function of the sample values $M(f_i, t_j)$ and local statistics of the data.

In the sliding-window approach, $\mathbf{M}$ is divided into overlapping submatrices. At every iteration, the sliding window is moved by a constant step size (we have taken the step size to be equal to unity) across the data and a submatrix $\mathbf{M}_{F,T}$ it extracted from the data $\mathbf{M}$. A local threshold is computed and used to classify the measurement samples in $\mathbf{M}_{F,T}$. Since the classification is performed in overlapping submatrices, every element of $\mathbf{M}$ is classified more than once. However, this matrix is classified in the presence of a different set of neighboring matrix elements at every step. If there is a strong signal in the vicinity of a weak signal within the measurement data, there will be at least one submatrix that will contain the weak signal and not the strong signal. In that particular submatrix, the weak signal can correctly be identified. In this manner, the biasing effect caused by the high dynamic range of signals can also be reduced.

If the sliding window is of dimensions $l \times m$, then every measurement sample in $\mathbf{M}$ will be classified Y times, where $Y = l \cdot m$. The independent classifications $v(k)$ of a measurement sample can be combined to obtain the final vote as

$$v_{\text{net}} = \frac{1}{Y} \sum_{k=1}^{Y} v(k) \tag{17}$$

where $v(k)$ denotes the classification of the measurement sample determined in the kth iteration of the windowing algorithm. A final decision on the classification of the sample can then be made based on one of the following criteria specified for v_{net}.

- *Simple combining criterion:* According to this criterion, $M(f_i, t_j)$ is classified as a signal only if $v_{\text{net}} > 0$.
- $n\%$ *majority criterion:* $M(f_i, t_j)$ is a signal only if $v_{\text{net}} \geq n/100$.
- *Super majority criterion:* $M(f_i, t_j)$ is a signal only if $v_{\text{net}} = 1$.

It can be seen that the simple combining criterion is the least stringent one, while the super majority criterion is the most stringent one among the criteria mentioned. A more stringent combining criterion yields a lower miss rate, at the expense of a high false-alarm rate. The different types of sliding windows that can be used are shown in Fig. 4. The submatrix $\mathbf{M}_{F,T}$ at each iteration is defined as $\mathbf{M}_{F,T} = [M(f_i, t_j)]$, where

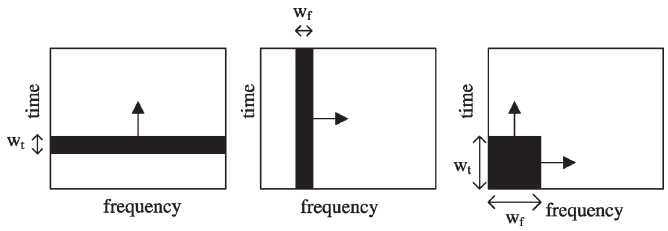

Fig. 4. Various types of sliding windows moved along (a) time, (b) frequency, and (c) both time and frequency.

$f_i \in F$, and $t_j \in T$. When a sliding window of width w_t is moved across time, F is the range of frequency channels in the bandwidth $[F_{\text{start}}, \ldots, F_{\text{stop}})$, and T is a subrange of the range $[T_{\text{start}}, \ldots, T_{\text{stop}})$, which spans w_t time instants every iteration. As a result, the total number of iterations will be $N_t - w_t + 1$. In the case of a sliding window of width w_f moving along the frequency dimension, F is a subrange of $[F_{\text{start}}, \ldots, F_{\text{stop}})$, which spans w_f frequency channels every iteration. The variable T represents the entire measurement time range $[T_{\text{start}}, \ldots, T_{\text{stop}})$. In this case, the total number of iterations will be $N_f - w_f + 1$. When using a sliding window of dimensions $w_f \times w_t$, F and T are subranges of the full frequency range and time range, respectively. In this case, the total number of iterations will be $(N_f - w_f + 1) \times (N_t - w_t + 1)$.

After the spectrum data pass through the first two stages of the processing and analysis block (see Fig. 2), they enter the final stage, which involves analysis of the processed data. The next section describes the characterization of the spectrum behavior, which involves data analysis followed by spectrum modeling.

IV. Characterization of Spectrum Utilization

The spectrum behavior can be characterized in terms of a set of parameters that can be determined via the analysis of processed measurements. In turn, these extracted parameters can be incorporated into a model for the spectrum measurements. The characterization can be a function of the receiver properties and the decision threshold. For effective dynamic spectrum management [21], the characterization of the spectrum is done on a channel-by-channel basis.

A. Analysis of Spectrum Measurements

The following *spectrum utilization parameters* (SUPs) can be determined from the measurements:

1) statistics of temporal channel availability and available bandwidth;
2) ambient noise power;
3) signal and transmitter characteristics such as received signal power, duty cycle, "on" and "off" times of a bursty signal, bandwidth, and transceiver mobility.

The statistics of the channel and bandwidth availability serve as an indication of the potential capacity (bandwidth–time) that can be supported by the underutilized spectrum [6] and allow for the prediction of future spectrum availability [15]. In addition, these statistics indicate the minimum frequency and time agility that is required by the radios for DSA operation [22]. The noise statistics can be used to determine the signal power that has to be transmitted for a specified percentage of the time to maintain a fixed received SNR [23], as well as determine the required receiver sensitivity. The features of the primary signal can be used for the process of classification. The duty cycle and the transceiver mobility specify the minimum rate at which the channel needs to be sensed for primary signal detection. On comparing the mean and maximum power levels among the measurements collected in a certain frequency channel, we can infer the signal power fading characteristics and the transceiver mobility [6]. The range of the spectrum measurements specifies the minimum dynamic range required by the receiver [6].

The matrix $\mathbf{M}$, in conjunction with $\mathbf{M}_c$, can be used to extract samples of the parameters. The probability distributions of the parameters can be computed from these samples, and from these distributions, we can estimate statistics such as the mean and variance. If K is the total number of signal occurrences in the channel, then the probability that the ith channel is available is given as

$$P_1^i = \frac{K}{N_t}, \qquad \text{where} \quad K = \sum_{j=1}^{N_t} M_c(f_i, t_j). \tag{18}$$

Samples of the signal and noise power can be extracted by analyzing a column vector of the spectrum measurements from channel f_i, along with their classifications, i.e., $\{M(f_i, t_j), M_c(f_i, t_j)\}$ is given.

Let the spectrum measurement (expressed in decibel meters) be transformed to the linear scale as

$$M_l(f_i, t_j) = 10^{M(f_i, t_j)/10} \text{ (mW)} \tag{19}$$

and let the decision threshold in linear scale be computed as

$$\eta_l((f_i, t_j) = 10^{\eta(f_i, t_j)/10} \text{ (mW)}. \tag{20}$$

Note that $\eta(f_i, t_j)$ can either be the local or global threshold used to classify $M(f_i, t_j)$ or be the average noise level across the channels adjacent to the signal frequency. The methods presented in Section III-A can be used to compute the threshold. By noting that a spectrum measurement that has been classified as a signal has both a signal and a noise component, a set of K samples of the signal power can be extracted from the data

$$S(f_i) = \{s(k) \,|\, s(k) = M_l(f_i, t_j) - \eta_l(f_i, t_j)\} \qquad \forall\, t_j$$

where

$$M_c(f_i, t_j) = 1 \qquad \text{for} \quad k = 1, 2, \ldots, K. \tag{21}$$

Moreover, the noise power samples can be extracted as

$$N(f_i) = \{n(r) \,|\, n(r) = M_l(f_i, t_j)\} \qquad \forall\, t_j$$

where

$$M_c(f_i, t_j) = 0 \qquad \text{for} \quad r = 1, 2, \ldots, N_t - K. \tag{22}$$

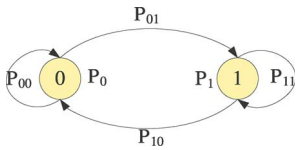

Fig. 5. Markov model of channel occupancy states.

Equations (21) and (22) represent the process by which the signal and noise components of a measurement sample are extracted with the help of the threshold $\eta_l\,(f_i, t_j)$, which serves as an estimate of the noise power. In fact, this process closely follows the model for the spectrum measurements proposed in Section IV-B.

The extracted samples can be used to compute several statistics such as the mean, standard deviation, dynamic range (equal to $\max\{S(f_i)\} - \min\{S(f_i)\}$), and threshold crossing rate $(P(N(f_i) \geq n)$ of the noise power. For instance, the SNR can be computed as

$$\text{SNR}(f_i) = 10\log_{10}\left(\frac{\overline{S}(f_i)}{\overline{N}(f_i)}\right)$$

where

$$\begin{aligned}\overline{S}(f_i) &= \text{Mean}\,\{S(f_i)\}\\ \overline{N}(f_i) &= \text{Mean}\,\{N(f_i)\}\,.\end{aligned} \tag{23}$$

The signal bandwidth can be determined by identifying the signal edges from a row vector of the classified spectrum data in the matrix $\mathbf{M}_c$. In a similar manner, given a column vector from $\mathbf{M}_c$, the start and stop times of signal transmissions can be identified to determine the "on" and "off" times of the signals.

B. Modeling of Spectrum Measurements

The extracted SUPs can be incorporated into the proposed model of the spectrum measurements that characterizes both the dynamics of the spectrum occupancy and the primary signal characteristics. In this model, a spectrum measurement is represented as a function of its components, namely, the signal $S(f_i, t_j)$, noise $N(f_i, t_j)$, and channel occupancy $M_c(f_i, t_j)$, which is given as

$$M(f_i, t_j) = (M_c(f_i, t_j) \times S(f_i, t_j)) + N(f_i, t_j). \tag{24}$$

Each component can be modeled as a random variable. In this manner, the proposed model can incorporate the individual models of the signal, noise, and channel occupancy into one comprehensive model for the spectrum. For instance, the channel occupancy can be modeled by a two-state Markov chain, as shown in Fig. 5. Extracting a column from the classified measurements matrix $M_c(f_i, t_j)$ yields the channel occupancy for a particular frequency channel f_i over the entire duration of the measurements. The parameters of the Markov model, namely, the state probabilities denoted by P_0 and P_1 corresponding to the states "0" and "1" and the state transition probabilities P_{00}, P_{01}, P_{10}, and P_{11}, can then be computed from this vector of temporal channel states.

TABLE I
COMPARISON BETWEEN GROUND-TRUTH AND MEASUREMENT CLASSIFICATIONS. VARIABLES a, b, c, AND d REPRESENT THE NUMBER OF TALLIES BETWEEN THE MEASUREMENT CLASSIFICATIONS AND THE GROUND TRUTH

		Data Classification	
		Signal	Noise
Ground Truth	Signal	a	b
	Noise	c	d

Having described the various components of SSF, the next section presents the results of applying the proposed processing techniques on real-world spectrum measurements that have been collected using our measurement subsystem.

V. PERFORMANCE EVALUATION OF PROPOSED PROCESSING TECHNIQUES

To evaluate the efficacy of the SSF and compare the performance among different implementations of this framework, a uniform performance evaluation procedure is required. The processed data that appear at the output of the classification algorithm are compared with the *ground truth* (see Table I). The ground truth obtained from a reliable source represents knowledge about the true presence or absence of a signal at a particular frequency and time instance [1]. The Federal Communications Commission website provides a database of all the radio stations near the measurement site at Lawrence, KS. These data can be used to create a matrix of the same dimensions as $\mathbf{M}$, where the columns that correspond to active radio channel frequencies are populated with 1s, while the remaining columns are populated with 0s. The decision made by the classification algorithm may (respectively, may not) conform with the ground truth, which results in correct (respectively, incorrect) classification. A *false alarm* occurs when a noise sample has incorrectly been classified as signal, and a *miss detection* occurs when a signal sample has incorrectly been classified as noise. These performance parameters can be computed as

$$\text{FA}(\%) = \frac{c}{c+d} \times 100 \tag{25}$$

$$\text{Miss Rate}(\%) = \frac{b}{a+b} \times 100 \tag{26}$$

where a, b, c, and d represent the count of the joint occurrences of the variables, as shown in Table I.

The processing techniques have been applied on spectrum measurements, which were collected in the Information and Telecommunications Technology Center, University of Kansas, Lawrence, over a 24-h period. The bandwidth resolution and the binwidth have been set to 10 kHz. Whereas all the measurements have been collected with a preset attenuation of 10 dB, the cellular band measurements were collected with 0-dB attenuation. Three types of spectrum bands have been targeted: 1) bands with fixed channelization such as the FM and TV broadcast bands; 2) bands occupied by digital "on/off" signals such as the 929–931-MHz paging band; and 3) the band with signals that occur very close to the noise level, such

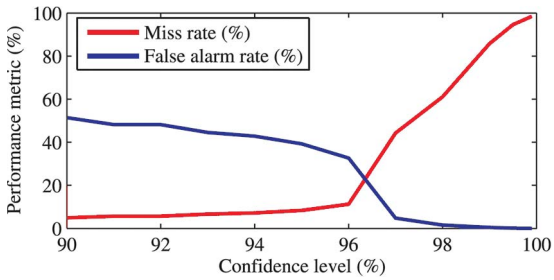

Fig. 6. Miss rate and false-alarm rate of the ROHT classification of FM band data with $\epsilon = 0.5$ for various confidence levels.

as the 824–849-MHz cellular band. In this paper, real-world measurement data have been used to test the proposed signal processing algorithms, as against using synthetic data generated through computer simulations.

In this section, the following key has been used to refer to the data-enhancement operations: η_l and η_r refer to the power levels of the noise and signal clipping, and $L = x$ refers to a cascade of the averaging filter and the Gaussian filter where the length of each filter is x.

A. FM Radio Spectrum: 88–108 MHz

The FM spectrum measurements (88–108 MHz) have been preprocessed with the following parameters: $\eta_r = -55$ dBm, $\eta_l = -98$ dBm, and $L = 4$. The results of the ROHT classification with $\epsilon = 0.5$ for various values of the confidence level are illustrated in Fig. 6. From this figure, we can infer that there is a tradeoff between the miss rate and false-alarm rate and that good results can be obtained for the FM band by operating the algorithm at around 96% confidence level.

The sliding-window approach employing a simple combining criterion was used with the ROHT algorithm on the preprocessed data. There was little improvement in the results by using the sliding window moved across time, as compared with the case where a sliding window was not used. The reason for this observation is described as follows. All the sweeps of measurement data (each row in $\mathbf{M}$) possess similar statistical properties since the occupancy in the FM band does not vary over time. By increasing the window size along time, the number of sweeps of data available for the local threshold (estimated for each submatrix $\mathbf{M}_{F,T}$) estimation increases. However, this results in an increase of redundancy in the data, which does not substantially improve the classification results.

In the case of the window moved along frequency and the square window, as shown in Fig. 7, there is an improvement in the performance when the window size is 15 or greater. The reason for this observed trend is explained as follows. In the FM band, the signals occupy a bandwidth of 150 kHz such that the spectrum measurements at 15 consecutive frequency steps, which coincide with a station band, represent samples of the signal power. The measurements from the adjacent guard bands represent samples of noise power. If a window with a width of less than 15 is employed, then as the window is moved across the frequency in $\mathbf{M}$, there will be instances when the window overlaps over data consisting of only the signal measurements. In this case, the classification of the windowed measurements

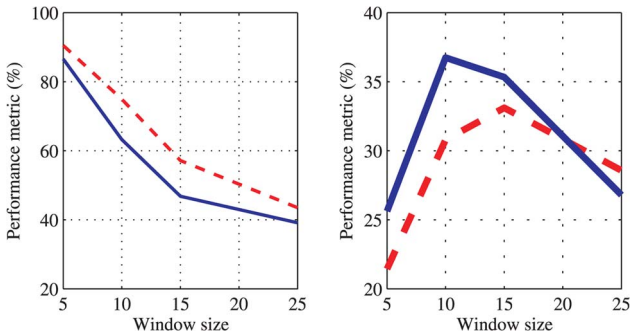

Fig. 7. Results of the ROHT algorithm used with the sliding-window approach on enhanced FM band data. (Left) Miss rates and (right) false-alarm rates. The dotted curve represents the case of a strip slided along frequency, and the solid curve represents the case when a square window has been used.

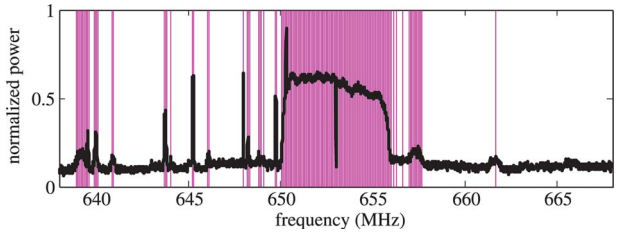

Fig. 8. Digital television band (638–668 MHz). (Black) Mean power spectrum and (magenta) its ROHT (95% confidence level and $\epsilon = 1.5$) classification.

results in the incorrect identification of noise, which is not really present. In a similar manner, the classification of measurements from the vacant portion of the FM spectrum results in the incorrect identification of the signals.

B. Digital TV Band: 638–668 MHz

In one of our measurement campaigns [24], measurements were collected from the analog (198–228 MHz) and the digital TV spectrum (638–668 MHz) at a distance of 200, 600, and 5000 ft from the TV tower. In Figs. 8 and 9(b), the presence of spurious signals and intermodulation products is clearly seen from the measurements collected at 200 ft from the tower. Fig. 8 shows the result of applying the ROHT (95% confidence level and $\epsilon = 1.5$) algorithm on time-averaged data, with the channel-44 signal (650–656 MHz) having correctly been classified. However, the spurious signals that include intermodulations have been mistaken to be signals.

C. Analog TV Band: 198–228 MHz

In Fig. 9(a), it is observed that the noise level varies with frequency. A sliding-window approach for data classification can improve the results. The results of applying the ROHT algorithm (96% confidence level and $\epsilon = 0.5$) on time-averaged data with and without a sliding window of width $= 2000$ that is moved along frequency are shown in Fig. 9(b) and (c). In the latter case, a 20% combining criterion was employed. Compared with Fig. 9(b) and (c), the results are improved in Fig. 9(c).

The analog TV measurements collected 200 ft from the tower were averaged and classified using Otsu's algorithm with the

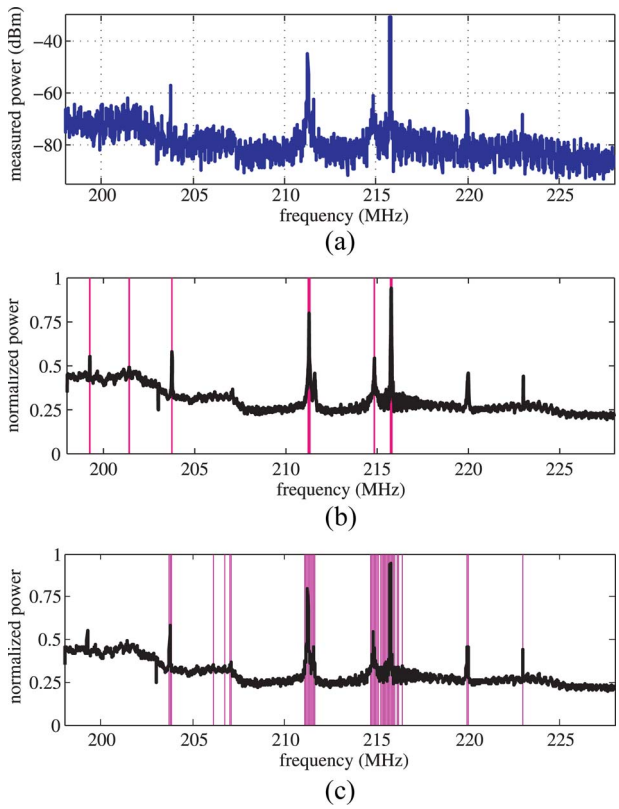

Fig. 9. Analog TV band (198–228 MHz). (Black) Mean power spectrum and (magenta) ROHT classification with 96% confidence and $\epsilon = 0.5$. (a) Instantaneous power spectrum of the analog TV band (198–228 MHz). (b) Classification using ROHT. (c) ROHT classification using a sliding window of width 2000 moved along frequency (20% criterion used).

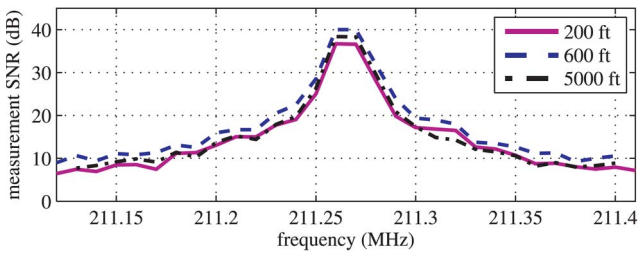

Fig. 10. SNR of analog TV signal at 211.13 MHz at various distances from the TV tower.

sliding window moved along frequency (window size $= 1300$). The feature-extraction tools were applied to the classified data, and the mean noise level was found to be -75.06 dBm with a standard deviation of 4.6311. The maximum and minimum noise power levels were -60.65 and -85.29 dBm. Data analysis was also performed to plot the SNR of the TV signal at 211.13 MHz at various distances from the tower (see Fig. 10). The bandwidth of this signal was found to be 0.31 MHz.

D. Paging Band: 929–931 MHz

To demonstrate the feature extraction tools, the measurements along the 930.04-MHz channel were first classified using Otsu's algorithm (see Fig. 11). By analyzing the classified data, the mean "on" time of the signals occupying the channel was

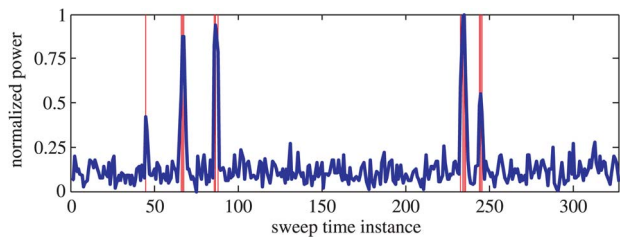

Fig. 11. Measurements from a 930.04-MHz channel classified by Otsu's algorithm.

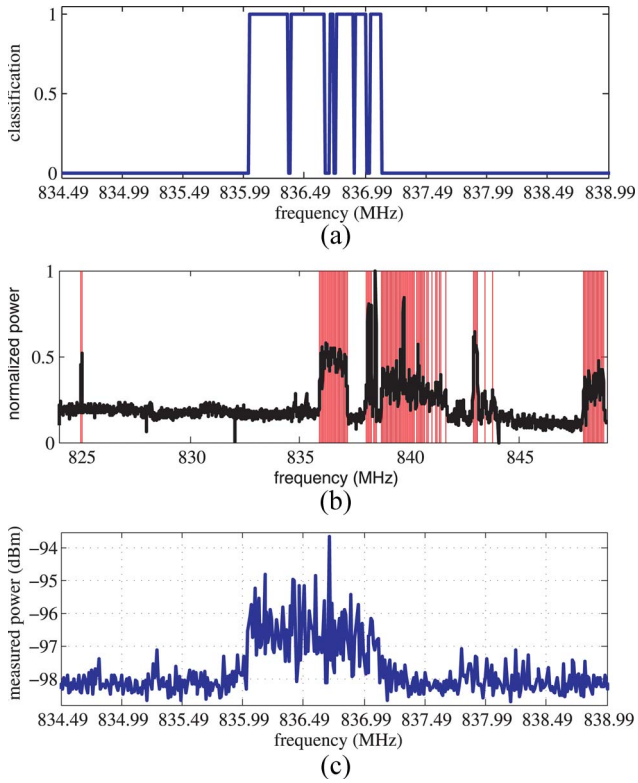

Fig. 12. Cellular band (824–849 MHz). (Black) Mean power spectrum and (magenta) classification. (a) Instantaneous power spectrum of the cellular band (834.49–838.99 MHz). (b) Classification of data after ROHT (96% confidence and $\epsilon = 0.5$) classification and median filtering. (c) Classification using Otsu's algorithm.

computed as $3.8T_s$, where T_s is the time resolution of the measurements.

When applied to the paging band (929–931-MHz) data, the ROHT algorithm with 99.5% confidence level and $\epsilon = 1.5$ gave the same performance as Otsu's algorithm. In these data, the dynamic range of the signals is small; thus, a higher confidence level and a higher ϵ has been used to avoid false alarms. This shows that the confidence level and ϵ are dependent on the dynamic range of the signals present in the data.

E. Cellular Band: 824–849 MHz

The measurements collected from the cellular band (824–849 MHz) were classified using the ROHT algorithm with 96% confidence and $\epsilon = 0.5$, followed by median filtering. Fig. 12(a) and (b) shows a sweep of the data before and after the classification. Otsu's algorithm gave nearly 100% miss

detection, even when used with noise filtering. However, when applied to the averaged spectrum measurements, it gave good results [see Fig. 12(c)].

While using a sliding window along with Otsu's algorithm on time-averaged data, a window size of 500 gave very high false-alarm rate, while a window size of 1000 gave decent results. This indicates that the window size depends on the occupancy of the band under consideration. A band with low occupancy is prone to false alarms when classification is performed. However, this can be reduced by using a sliding-window approach with a suitable window size such that every subset of the data that are extracted by the sliding window contains signals.

F. Summary of Results

The results achieved on the FM band measurements were not as good as the results obtained with the other data sets. In fact, the FM band data represent the worst-case scenario for several reasons. The FM band data was collected at close proximity from the transmission tower for the radio station KJHK 90.7 MHz. Hence, the presence of intermodulations and local-oscillator sideband noise is expected. In addition, there are weak signals that occur close to the noise level, and these may not be identified by the classification algorithms. Furthermore, the dynamic range of the measurements is high.

Time averaging improved the performance of the classification algorithms when applied to the bands with fixed channelization, such as the FM band and the TV bands. However, time averaging did not perform well when applied to the paging band due to the random nature of the channel occupancy in this band.

The ROHT and Otsu's algorithms performed well on all the bands with the help of time averaging. However, the ROHT algorithm was found to possess some drawbacks. The parameters of the ROHT algorithm had to be set depending on the dynamic range of the signal. In addition, the ROHT algorithm requires a large number of samples for estimating the threshold. This was observed when the performance on the FM band data improved by increasing the window size while using a sliding-window approach.

The sliding-window approach improved the results of the classification algorithms. However, in the case of the cellular band, which is sparsely occupied, smaller window sizes of less than 1000 gave high false alarms. This exposed a drawback that the window size has to be set according to the occupancy of the target band.

VI. Conclusion

The proposed framework has introduced standardization to spectrum surveying, which can enable collaborations on studying the spectrum behavior. SSF is expected to aid in the research of DSA networks and provide the necessary statistics needed for spectrum policy reforms. The proposed framework has been used to study the feasibility of secondary usage in the TV spectrum [24] and incorporated into a novel spectrum sensing architecture [8].

Techniques have been proposed to counter the various challenges to the spectrum measurements. In this paper, the proposed algorithms have been tested and evaluated by directly applying them on real-world spectrum measurements. This approach provides true results, as opposed to results that are obtained through mathematical analysis. With the exception of the FM band data, good measurement classification results were obtained when the techniques were applied on data collected from the TV bands, the paging band, and the cellular band. Although the proposed methods have been found to be reliable, they possess the drawback that they cannot distinguish between signal, noise, and interference. In addition, it has been observed that the parameters of the proposed ROHT algorithm and the sliding-window algorithm depend on the occupancy of the band and the dynamic range of the signals. As a result, some prior knowledge of the spectral occupancy in the band of interest may be required to apply these algorithms.

The proposed framework has primarily been designed for offline spectrum measurement processing. The proposed ROHT algorithm and its sliding-window version have been found to perform well when applied on a large set of measurements. In addition, the spectrum data preprocessing and sliding-window classification methods operate on a data set and not on a sample-by-sample basis. Hence, in the proposed form, the classification methods may not be suited for real-time spectrum sensing in DSA networks. Second, the *a priori* knowledge of the target spectrum required for optimum classification may not be available in cognitive radio networks that operate in an automated manner.

A set of parameters of spectrum utilization were identified and tools have been developed in Matlab to extract these features from the processed data. A comprehensive model for the spectrum measurements has also been presented.

Acknowledgment

The authors would like to thank T. Weidling and R. Petty for developing the *Spectrum Miner* software and Matlab tools to retrieve the spectrum data from the spectrum repository and making a significant contribution to the development of the ROHT algorithm. In this submission, the data-enhancement and characterization stages of the proposed framework, the proposed adaptive thresholding, and the results have not previously been published.

References

[1] F. Weidling, D. Datla, V. Petty, P. Krishnan, and G. J. Minden, "A framework for RF spectrum measurements and analysis," in *Proc. IEEE Int. Symp. New Frontiers Dyn. Spectrum Access Netw.*, Baltimore, MD, Nov. 2005, pp. 573–576.

[2] A. J. Petrin, "Maximizing the utility of radio spectrum: broadband spectrum measurements and occupancy model for use by cognitive radio," Ph.D. dissertation, School Elect. Comput. Eng., Georgia Inst. Technol., Atlanta, GA, Aug. 2005.

[3] A. Petrin and P. G. Steffes, "Analysis and comparison of spectrum measurements performed in urban and rural areas to determine the total amount of spectrum usage," in *Proc. Int. Symp. Adv. Radio Technol.*, Boulder, CO, Mar. 2005, pp. 9–12.

[4] A. Petrin and P. G. Steffes, "Study of spectrum usage and potential interference to passive remote sensing activities in the 4.5 cm and 21 cm bands," in *Proc. IEEE Int. Geosci. Remote Sens. Symp.*, Anchorage, AK, Sep. 2004, vol. 3, pp. 1679–1682.

[5] J. R. Hoffman and R. J. Matheson, "RSMS measurement and analysis of LMR channel usage," in *Proc. Int. Symp. Adv. Radio Technol.*, Boulder, CO, Mar. 2005, pp. 13–19.

[6] S. Ellingson, "Spectral occupancy at VHF: Implications for frequency-agile cognitive radios," in *Proc. IEEE Veh. Technol. Conf.*, Dallas, TX, Sep. 2005, vol. 2, pp. 1379–1382.
[7] M. A. McHenry, "NSF spectrum occupancy measurements project summary," Shared Spectrum Co., Vienna, VA, Tech. Rep., Aug. 2005.
[8] D. Datla, R. Rajbanshi, A. M. Wyglinski, and G. J. Minden, "Parametric adaptive spectrum sensing framework for dynamic spectrum access networks," in *Proc. 2nd IEEE Int. Symp. New Frontiers Dyn. Spectrum Access Netw.*, Dublin, Ireland, Apr. 2007, pp. 482–485.
[9] A. Petrin and P. G. Steffes, "Measurement and analysis of urban spectrum usage," in *Proc. Int. Symp. Adv. Radio Technol.*, Boulder, CO, Mar. 2004, pp. 45–48. NTIA Special Pub. SP-04-409.
[10] G. F. Gott, S. K. Chan, C. A. Pantjiaros, and P. J. Laycock, "High frequency spectral occupancy at the solstices," *Proc. Inst. Elect. Eng.—Commun.*, vol. 144, no. 1, pp. 24–32, Feb. 1997.
[11] C. A. Pantjiaros, P. J. Laycock, G. F. Gott, and S. K. Chan, "Development of the Laycock-Gott occupancy model," *Proc. Inst. Elect. Eng.—Commun.*, vol. 144, no. 1, pp. 33–39, Feb. 1997.
[12] D. J. Percival, M. Kraetzl, and M. S. Britton, "A Markov model for HF spectral occupancy in Central Australia," in *Proc. 7th Int. Conf. High Frequency Radio Syst. Tech.*, Nottingham, U.K., Jul. 1997, pp. 14–18.
[13] D. Cabric, S. M. Mishra, and R. W. Brodersen, "Implementation issues in spectrum sensing for cognitive radios," in *Proc. 38th Asilomar Conf. Signals, Syst., Comput.*, Pacific Grove, CA, Nov. 2004, vol. 1, pp. 772–776.
[14] R. Tandra and A. Sahai, "Fundamental limits on detection in low SNR under noise uncertainty," in *Proc. Int. Conf. Wireless Netw., Commun. Mobile Comput.*, 2005, vol. 1, pp. 464–469.
[15] S. D. Jones, N. Merheb, and I.-J. Wang, "An experiment for sensing-based opportunistic spectrum access in CSMA/CA networks," in *Proc. IEEE Int. Symp. New Frontiers Dyn. Spectrum Access Netw.*, Baltimore, MD, Nov. 2005, pp. 593–596.
[16] N. Otsu, "A threshold selection method from gray-level histograms," *IEEE Trans. Syst., Man, Cybern.*, vol. SMC-9, no. 1, pp. 62–66, Jan. 1979.
[17] M. Sonka, V. Hlavac, and R. Boyl, *Image Processing, Analysis and Machine Vision*, 2nd ed. Pacific Grove, CA: Brooks/Cole.
[18] M. Cheriet, J. N. Said, and C. Y. Suen, "A recursive thresholding technique for image segmentation," *IEEE Trans. Image Process.*, vol. 7, no. 6, pp. 918–921, Jun. 1998.
[19] S. O. Rice, "Mathematical analysis of random noise," *Bell Syst. Technol. J.*, vol. 24, pp. 46–156, 1945.
[20] M. Pagano and K. Gauvreau, *Principles of Biostatistics*, 2nd ed. Pacific Grove, CA: Duxbury, Mar. 2000.
[21] XG Working Group, "The XG architectural framework: Request for comments," BBN Technol., Cambridge, MA. ver. 1.0, Tech. Rep.
[22] M. McHenry, "Spectrum measurements to support dynamic spectrum sharing research and development," presented at the National Science Foundation (NSF) Future Spectrum Technology Policy Workshop, Washington, DC, May 25–27, 2005.
[23] M.-H. Chang and K.-H. Lin, "A comparative investigation on urban radio noise at several specific measured areas and its applications for communications," *IEEE Trans. Broadcast.*, vol. 50, no. 3, pp. 233–243, Sep. 2004.
[24] R. Rajbanshi, V. R. Petty, D. Datla, F. Weidling, D. DePardo, P. Kolodzy, M. J. Marcus, A. M. Wyglinski, J. B. Evans, G. J. Minden, and J. A. Roberts, "Feasibility of dynamic spectrum access in underutilized television bands," in *Proc. 2nd IEEE Int. Symp. New Frontiers Dyn. Spectrum Access Netw.*, Dublin, Ireland, Apr. 2007, pp. 331–339.

Dinesh Datla (S'07) received the B.E. degree in electronics and communications from the University of Madras, Chennai, India, in 2004 and the M.S. degree in electrical engineering from the University of Kansas, Lawrence, in 2007. He is currently working toward the Ph.D. degree in electrical engineering with the Department of Electrical and Computer Engineering, Virginia Polytechnic Institute and State University, Blacksburg.

He was with the Information and Telecommunication Technology Center, University of Kansas, where his research focused on the measurement, analysis, and modeling of the radio frequency spectrum utilization and efficient scheduling for spectrum sensing. His current research interests include next-generation radio systems such as software radio and cognitive radio.

Alexander M. Wyglinski (S'99–M'05) received the B.Eng. degree in electrical engineering from McGill University, Montreal, QC, Canada, in 1999, the M.S.(Eng.) degree in electrical engineering from Queen's University, Kingston, ON, Canada, in 2000, and the Ph.D. degree in electrical engineering from McGill University in 2005.

From 2005 to 2007, he was an Assistant Research Professor with the Information and Telecommunication Technology Center, University of Kansas, Lawrence. He is currently an Assistant Professor with the Department of Electrical and Computer Engineering, Worcester Polytechnic Institute (WPI), where he is a Codirector of the WPI Limerick Project Center and the Director of the Wireless Innovation Laboratory. He is very actively involved in the wireless communication research community, particularly in the fields of cognitive radio systems and dynamic spectrum access networks. His current research interests are in the areas of wireless communications, wireless networks, cognitive radios, software-defined radios, transceiver optimization algorithms, dynamic spectrum access networks, spectrum-sensing techniques, machine-learning techniques for communication systems, signal processing techniques for digital communications, hybrid fiber–wireless networking, and both multihop and ad hoc networks.

Dr. Wyglinski was a member of the IEEE Communications Society, the IEEE Signal Processing Society, the IEEE Vehicular Technology Society, IEEE Women in Engineering, and Sigma Xi. He served as a Guest Coeditor for the *IEEE Communications Magazine* with respect to two feature topics on cognitive radio (May 2007 and April 2008) and currently serves on the editorial boards of the *IEEE Communications Magazine* and IEEE COMMUNICATIONS SURVEYS AND TUTORIALS. He was a Technical Program Committee Cochair of the Second International Conference on Cognitive Radio Oriented Wireless Networks and Communications, the Track Chair for the 64th and 66th IEEE Vehicular Technology Conference, a Tutorial Cochair for the 2008 IEEE Symposia on New Frontiers in Dynamic Spectrum Access Networks (IEEE DySPAN 2008), and the Wireless Mobile Communications Track Chair of the 2008 IEEE Military Communications Conference. He is the Communications Techniques and Technologies Track Cochair of the 2009 IEEE Military Communications Conference and is currently the Student Travel Grants Chair for the 2010 IEEE DySPAN. He is a Technical Program Committee Member for numerous IEEE and other international conferences in wireless communications and networks.

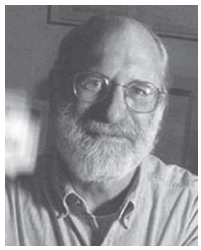

Gary J. Minden (SM'01) received the B.S.E.E. and Ph.D. degrees from the University of Kansas, Lawrence, in 1973 and 1982, respectively.

From 1978 to 1980, he was a Vice President of CHILD, Inc., where he was a Codesigner of the LIGHT-50 computer graphic terminal. In 1981, he joined the Faculty of electrical engineering, University of Kansas, where he led the implementation of a new computer-engineering program. In 1991, he completed a sabbatical at Digital's System Research Center, working on gigabit local area networks. From June 1994 through December 1996, he was a Program Manager with the Defense Advanced Research Projects Agency Information Technology Office in the area of high-performance networking systems. He initiated a new research program in active networking. He has lead several research projects in high-performance wide area networks, mobile wireless systems, adaptive computational systems, and innovative networking protocols. He has served on three Defense Science Board Task Forces: Tactical Battlefield Communications task force, Spectrum Management task force, and Wideband RF Modulation task force, where he was the Chair. He is currently a Professor of electrical engineering and computer science with the Information and Telecommunication Technology Center, University of Kansas. His research interests are in the areas of large-scale distributed systems that encompass high-performance networks, mobile wireless networks, computing systems, and distributed software systems.

Dr. Minden is a member of the Association for Computing Machinery and the American Association for the Advancement of Science.